



Research Paper

Study on multi-effect distillation of seawater with low-grade heat utilization of thermal power generating unit

Yuan Xue^a, Xiaoze Du^{b,*}, Zhihua Ge^a, Lijun Yang^a^a Key Laboratory of Condition Monitoring and Control for Power Plant Equipment (North China Electric Power University), Ministry of Education, Beijing 102206, China^b School of Energy and Power Engineering, Lanzhou University of Technology, Lanzhou 730050, China

HIGHLIGHTS

- Exhaust flue gas of power plant boiler is used as heat source in LT-MED system.
- Three schemes are proposed to utilize low grade heat of power plant.
- Effect of extraction steam load variation on the thermal power plant is analyzed.
- Water-power cogeneration systems are economically analyzed.

ARTICLE INFO

Keywords:

Power boiler

Low grade heat utilization

Seawater desalination

Multi-effect distillation

ABSTRACT

In order to reduce the energy consumption of low temperature multi-effect distillation (LT-MED), three schemes were proposed to utilize the low-grade heat of thermal power unit. The LT-MED system was combined with the thermal power unit by abolishing gas–gas heater (GGH) to recover the waste heat of flue gas and utilize the recirculating seawater of steam turbine condenser. Physico-mathematical models were established, with which the fresh water production performance of each scheme was investigated. Comparing with the reference six-effect TVC-MED system, the coal consumption rate of power generation dropped by 6.05 g/kWh for a 600 MW power generating unit, as well as thousand tons fresh water production could be obtained by using the flue gas as the heat resource of the first effect. Economic analysis results showed that reduce the amount of extraction steam from the turbine can significantly reduce water production cost. From the viewpoint of coal consumption rate, the combination of exhaust flue gas with the LT-MED system was better than that of heating condensed water. The gained output ratio (GOR) can be effectively enhanced up to 12.79.

1. Introduction

Seawater desalination has been becoming an important way to relieve the threat from water shortages all over the world. At present, seawater desalination devices in the world can produce fresh water nearly 1 Mm³ a day, among which, reverse osmosis (RO) and low temperature multi-effect distillation (LT-MED) are the main desalination techniques [1]. Due to the top brine temperature (TBT) of early multi-effect distillation (MED) was about 100 °C, salt was easy to precipitate on the surface of the heat exchanger, which led to severe fouling problems. Compared with multi-stage flash distillation (MSF), MED has become uncompetitive in desalination industry in the past. Recently, the top brine temperature of LT-MED can be declined lower than 70 °C, which not only effectively solves the problems of scale and corrosion, but also simplifies the pretreatment of seawater and

improves the purity of fresh water. Hence, a rapid progress has been witnessed for LT-MED technique in the market of seawater desalination in recent years [2]. Numerous researches have been invested to decrease the energy consumption of the LT-MED process. The thermal vapor compressor (TVC) has to be combined with LT-MED because of its simple mechanical structure and its ability to make use of high grade energy of extracting source steam [3–5]. A number of papers have been presented in the literature regarding mathematical models and parameters analysis of MED with or without TVC [6–8]. The simulation results have shown a good agreement with realistic design data and operations.

The research of thermal desalination methods, especially for LT-MED, mainly focuses on the heat transfer and fouling characteristics within the heat exchanger [9], thermodynamic and thermoeconomic study of integrated desalination [10], and new system coupling

* Corresponding author.

E-mail address: duxz@ncepu.edu.cn (X. Du).

Nomenclature

A	heat transfer area, m ²
B	coal consumption, t/h
Bo	boiling number
BPE	boiling point elevation, °C
C_{annual}	water production cost, \$/m ³
C_{At}	total heat transfer area cost, \$
C_{cap}	annualized capital cost, \$/year
C_{CAP}	total capital cost, \$
C_{chem}	chemical cost, \$/m ³
C_{co}	construction cost, \$
C_d	direct capital cost, \$
C_{elec}	electrical power cost, \$/kWh
C_{em}	contingency cost, \$
C_{eq}	equipment cost, \$
C_{fr}	freight cost, \$
C_i	indirect capital cost, \$
C_{ins}	annual insurance cost, \$/year
C_{lab}	annual labor cost, \$/year
C_{land}	land cost, \$
C_{main}	maintenance cost, \$/m ³
C_{op}	annualized operational cost, \$/year
C_{ow}	owner cost, \$
C_p	specific heat at constant pressure, kJ/(kg·K)
C_{sd}	site development cost, \$
C_{steam}	motive steam cost, \$/ton
Co	convection number
CR	concentration ratio of seawater
D	distillate production rate, m ³ /day or Diameter, m
D_e	equivalent diameter, m
f	plant load factor
G	mass flux, kg/(m ² ·s)
GOR	gain output ratio, kg/kg
h	enthalpy, kJ/kg or Convective heat transfer coefficient, W/(m ² ·K)
i	interest rate
k	heat conductivity, W/(m·K)
$LTMD$	logarithmic heat transfer coefficient, °C
M	mass flow rate, kg/s
NEA	non-equilibrium allowance
n	number of years
P	turbine power or pressure, MW or Pa
PCF	pressure correction factor
PR	performance ratio
Q	heat transfer rate, kW
q	heat flux, W/m ²

R_{α}	entrainment ratio
R_{fi}	fouling resistance inside tube, (m ² ·K)/W
R_{fo}	fouling resistance outside tube, (m ² ·K)/W
Re_l	liquid Reynolds number
S_f	spacing of fins, m
S_1	windward tube spacing, m
S_2	tube spacing along wind direction, m
T	temperature, °C
TCF	temperature correction factor
U	overall heat transfer coefficient, kW/(m ² ·K)
w_{aux}	auxiliary power demand, kWh/m ³
X	salinity, %
x	dryness fraction
Z	amortization factor

Subscripts

b	brine
c	cold side or Condensing
$c4$	extracting steam of forth section
ce	exhaust condensed water from first effect
cq	extracting steam
cw	cooling water
d	distillate
ev	entrained vapor
f	feed water
h	heating medium
i	serial number of evaporator or The inside of tube
in	inlet
m	compressed vapor
MED	traditional MED-TVC system
mod	proposed modified system
n	number of evaporators
o	outlet or The outside of tube
pq	exhaust steam from turbine
s	steam
v	secondary vapor
w	condensate water
y	flue gas

Greek symbols

δ_f	fin thickness, m
λ	latent heat, kJ/kg
μ	dynamic viscosity, Pa·s

approach with renewable or waste heat source [11–13]. In the various combination of different desalination methods, Shahzad et al. presented experiments of an LT-MED and LT-MEDAD plants. It is observed that the hybrid system not only improves the performance ratio but also minimizes fouling and scaling on the tube surfaces [14]. Mokhtari et al. designed and analyzed a “Gas turbine + Multi effect desalination + Reverse Osmosis” system. The result showed that more fresh water could be derived from the whole system [15]. MSF-MED system has been demonstrated to be around 40%–50% better than the conventional MED process by Rahimi et al. [16]. Among different types of renewable energy, solar energy is one of the most important ways to integrate with desalination plant [17,18]. Many geothermal sources were also considered to be the heat sources of thermal desalination system [19]. Bundschuh et al. suggested that geothermal option is superior to the solar option to integrate with thermal-based desalination because it provided a constant heat source in contrast to solar [20]. The

waste heat from solid fuel or hot water as the heat source of thermal desalination is another research filed. Maheswari et al. conducted an experiment to utilize the wasted heat in exhaust flue gas of an internal combustion engine for desalination. The overall efficiency of the system was enhanced and about 3.0 l/h of saline water could be desalinated by utilizing the waste heat [21]. Zhang et al. installed and tested an LT-MED system which powered by the cooling water of diesel power generator and the system was well predicted by the thermodynamic model [22].

Large scale desalination is an energy intensive process and the energy consumption is the dominant part of fresh water cost. The important advantage of LT-MED is that low grade heat can be used as the heat source because its top brine temperature is less than 70 °C. Meanwhile, thermal power generation is the most efficient utilization pattern of fossil fuels. Nevertheless, significant portions of the energy during power generation process is discharged into the environment in

the form of low grade waste heat. It has been demonstrated that the waste heat of power plant can be complementary to the energy demand of thermal seawater desalination. Cogeneration of water and electricity can improve the energy utilization efficiency from the present 40% to more than 60% [23]. However, restricted by design and operation parameters of the steam turbine in a power plant, the steam temperature extracted from a typical 300 MW or larger capacity power generating unit is always above 320 °C, which causes a lot of high grade energy loss in the desalination process when it is used as the heat source of LT-MED system.

To avoid the waste of high-grade heat from the steam turbine, three different integrations that utilize flue gas to evaporate or preheat seawater are proposed in the present study. Based on the thermodynamic models, Engineering Equation Solver (EES) and Epsilon software are adopted to analyze the maximum freshwater productivity and the effect on the performance of power plant. Through economic analysis, the water production costs of different water-electricity cogeneration models were compared. As a comparison, the effect of the extracting steam amount of the coal consumption rate is analyzed under the condition that the extracting steam from steam turbine is used as the heat source of LT-MED, which is the traditional and present common approach of integration between seawater desalination and thermal power generation.

2. System description and physical model

The LT-MED process can be configured as forward, backward, or parallel feed, which differs in the directions of the heat source and the seawater. In the parallel flow layout, the pressure and temperature decrease in the vapor flow direction. The feed brine is divided into two shares after preheating in the condenser. As shown in Fig. 1, one is the cooling water of turbine condenser and ejected back to sea. The other is fed into individual effects equally as feed brine. Seawater enters in the first effect is heated to the boiling point by source steam. Only a portion of the seawater can be evaporated, the concentrated saltwater, indicated as feed brine of the next effect in Fig. 1, is fed into the second effect, where it flashes and mixes with the feed seawater. The vapor produced in the first effect is condensed after heating seawater in the second effect. The condensed water flows through a flash tank to produce more steam enter into the third effect. This process is repeated till the last effect. Due to the pressure in each effect is lower than the

previous one, the main advantage of parallel flow is the simplicity without pump between effects.

In forward feed, seawater and the heat source flow concurrently from the high temperature to the low temperature effect. Seawater enters the first effect, becomes partially evaporated, and flows to the next effect. The advantage is the absence of pumps for ejecting brine from the effects and the disadvantage is that all the feed has to be heated to the top boiling temperature.

Backward feed refers to that steam vapor and seawater flow in the opposite direction. Seawater is introduced into the last effect which has the lowest temperature and pressure within the system. The brine flows through successive effects towards the first effect by pump because of the increase of pressure and temperature across the effects, thus, causing serious system fouling because the highest temperature and salinity are found in the first effect. Backward feed also tends to increase the complexity and operational power consumption of the system because it requires pumps between effects [24].

With consideration of the three different configurations, research has shown that parallel/cross flow has higher GOR and better performance characteristics than the other two feed configurations [8]. Therefore, a physical model of parallel/cross flow is adopted in this study.

As an example of the parallel feed LT-MED system and a contrast of the present proposal, a schematic diagram of six effects LT-MED with TVC is shown in Fig. 1, in which the low pressure vapor of TVC is induced from the fourth effect.

In addition to the steam turbine, exhaust flue gas of the boiler in thermal power unit can also provide multiple-grade waste heats. At present, main uses of the waste heat of flue gas are preheating air, preheating and drying fuels, and heating condensate [25,26]. In order to improve the efficiency of power generating unit, the low temperature flue gas of the boiler between induced draft fan and desulfurization tower was usually utilized by the following two patterns. The first one is to heat the net gas by using flue gas heat exchanger (GGH). But it's prone to be heavy congestion [27], which results in flue gas desulfurization (FGD) system shutdown and problem such as water consumption increases. The other one is to heat condensed water by using the low temperature economizer [25]. At present, there are lots of power generating units without GGH that adopt wet chimneys to discharge flue gas. Investigations have shown that the method will not increase the local ground concentration of NO_x significantly [28]. Hence it's

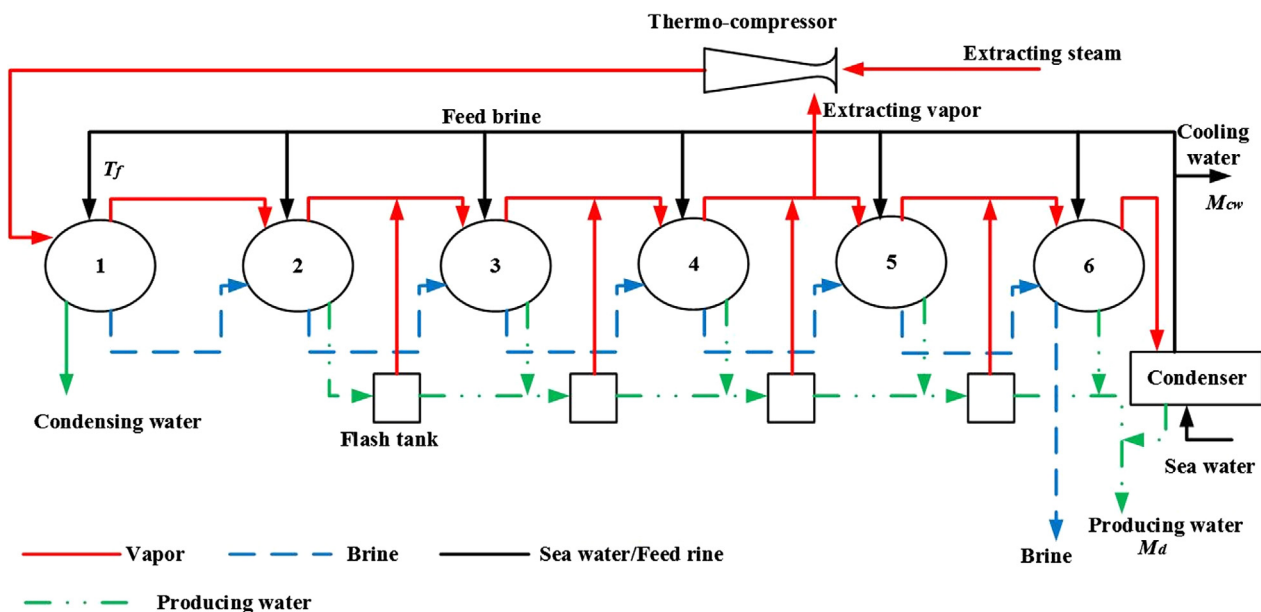


Fig. 1. Schematic diagram of six effects LT-MED system with TVC.

completely feasible to cancel GGH after the installation of denitration unit, which makes it is possible using the waste heat of exhaust flue gas as the heat source in LT-MED system. With the recovery of the heat of exhaust flue gas before flue gas desulfurizer, the extracted steam from the turbine that used as the heat source of desalination can be replaced and more output of power can be obtained. In some coal fired power plant, the cold source of the steam turbine condenser is circulating seawater. By using this part of seawater, the inlet temperature of desalination can be increased.

Based on the above analysis, in order to utilize the low grade heat of the power generating unit, three LT-MED schemes are proposed, which are indicated as Scheme 1, Scheme 2 and Scheme 3. The schematic diagram of scheme 1 and 2 is shown in Fig. 2, and the schematic diagram of scheme 3 is shown in Fig. 3.

Scheme 1: Use the exhaust flue gas as the heat source of the first effect of MED system. The parallel feed flow into the evaporator of each effect is preheated by the second vapor generated from the last effect.

Scheme 2: Use the exhaust flue gas as the heat source of the first effect of the MED system. Part of circulating seawater of the steam turbine condenser parallel flows into each effect as feed brine having been preheated by the second vapor generated from the last effect.

Scheme 3: Use the extracting steam from the turbine as the heat source of the first effect. The feed brine is sent into effects having been preheated by second vapor from the last effect, the condensed water of the first effect and exhaust flue gas successively.

3. Mathematical model

The following assumptions are adopted for analysis simplification and accuracy.

- (1) The properties of seawater are the function of temperature and concentration.
- (2) The properties of the produced fresh water and second vapor are the functions of temperature.
- (3) The salinity of the produced fresh water is ignored.
- (4) The steam condensation loss and flow friction loss in MED system are ignored.
- (5) The temperature of flue gas exhausted from the desalination system

is assumed constant at 85 °C.

- (6) The material for evaporator is assumed as the Cu/Ni 90/10 alloy (180 \$/m²).

3.1. Thermodynamic analysis

The thermodynamic mathematical models of the proposed system are listed in Table 1, including that of mass conservation, salt balance and energy balance for individual components, including that of evaporators, condensers, and ejector. The corresponding thermodynamic losses are listed in Table 2.

For the first effect, the mass conservation, salt balance, and energy balance are expressed as Eqs. (1), (3), (5) respectively. And for other effects, due to the brine of prior flows into the latter one to flash, the balance equations are expressed as Eqs. (2), (4), (6). The Q in Eq. (5) can be Q_y and $M_s \lambda_s$ when the heat medium is the exhaust flue gas or the extracting steam of turbine.

The Q in Eq. (7) is the heat transfer quantity in the condenser, which can be the released heat by vapor from last effect, $M_{d(n)} \lambda_{v(n)}$, flue gas heat capacity, Q_y , or the heat released by condensed water of first effect, $M_s C_p (T_s - T_{ce})$.

For the steam driven MED systems, the performance is evaluated by the standard gain output ratio, GOR, which is the ratio of the distillate production to the steam input, as expressed by Eq. (12). For the sensible heat source system, the performance ratio, PR, is far more general, where the amount of energy used for the evaporation of fresh water is compared against the initial energy input as Eq. (13). In Eq. (13), m_h is the mass flow rate of the heating medium, Δh_i is the specific enthalpy difference released by the heat source, and Δh_{ref} is the specific reference enthalpy of the distillate, $\Delta h_{ref} = 2336$ kJ/kg [30].

The heat exchangers used in this study can be classified as follows. The evaporator of the first effect can be a gas-evaporation heat exchanger when the heat source is exhaust flue gas. Or it can be a condensation-evaporation heat exchanger when the heat medium is steam just like other effects. The condenser is a condensation-liquid heat exchanger. Preheater can be either liquid-liquid or gas-liquid heat exchanger, such as in Scheme 3.

BPE is the boiling point elevation of feed brine during evaporation. $NEA_{(i)}$ and $NEA'_{(i)}$ are the non-equilibrium allowance in brine flash and distillate flash. Coal consumption variation due to the variation of extracting steam from the turbine of the power generating unit is expressed by Eq. (19).

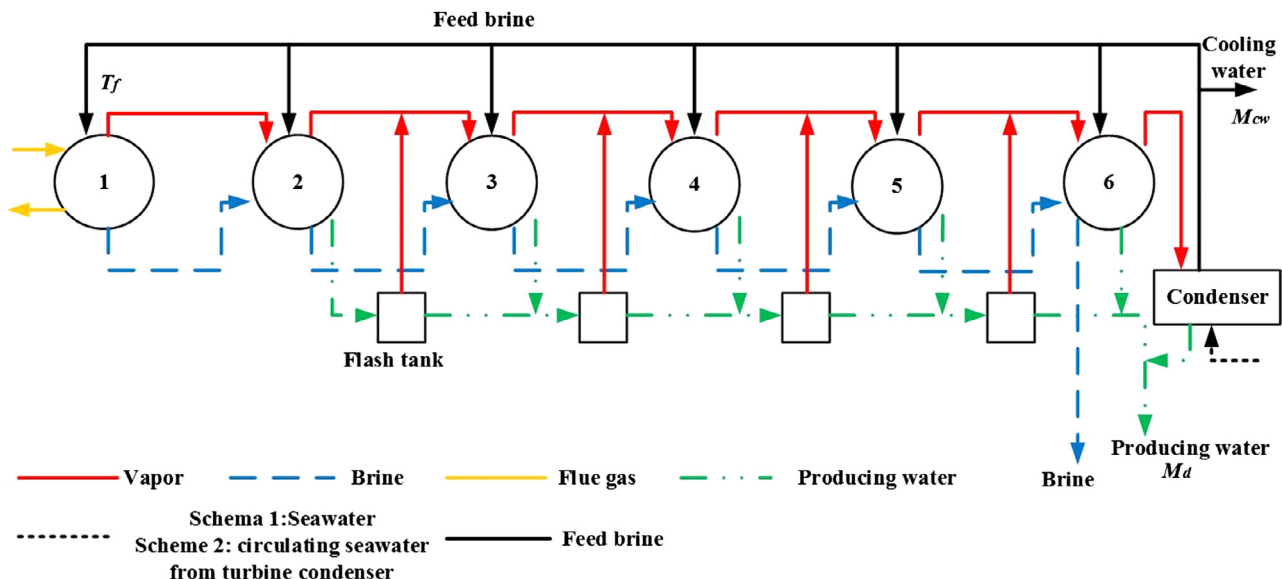


Fig. 2. Schematic diagram of scheme 1 and 2.

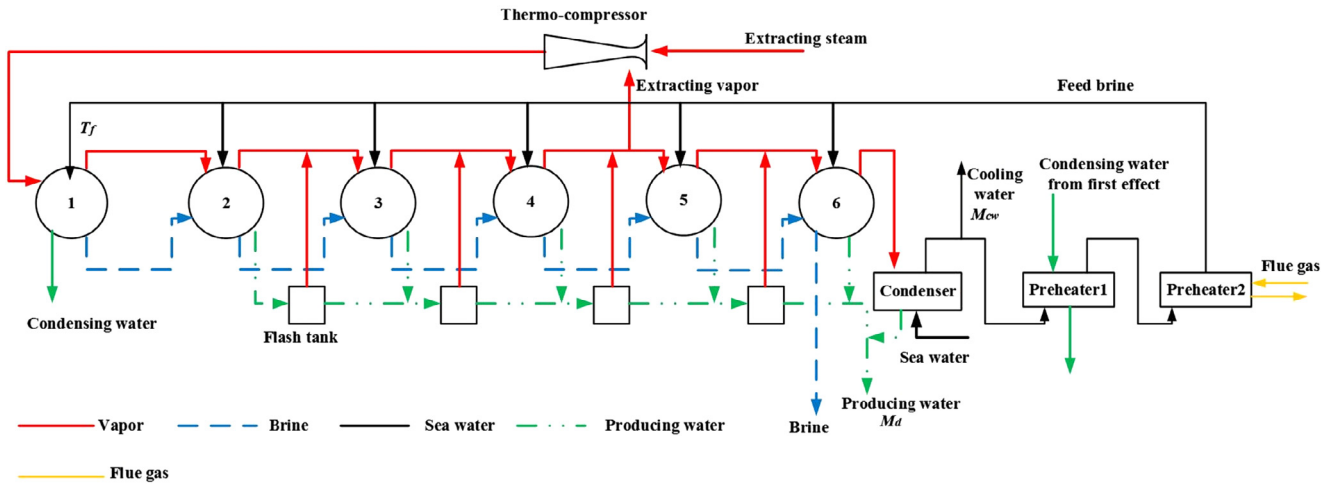


Fig. 3. Schematic diagram of scheme 3.

Table 1
Thermodynamic modeling of the proposed systems [29].

Parameters	Formulas	
Mass conservation in evaporator	$M_{f(i)} = M_{d(i)} + M_{b(i)}$	(1)
	$M_{f(i)} + M_{b(i-1)} = M_{d(i)} + M_{b(i)}$	(2)
Salt balance in evaporator	$M_{f(i)}X_{f(i)} = M_{b(i)}X_{b(i)}$	(3)
	$M_{f(i)}X_{f(i)} + M_{b(i-1)}X_{b(i-1)} = M_{b(i)}X_{b(i)}$	(4)
Energy balance in evaporator	$Q = M_{f(i)}C_{p(i)}(T_{b(i)} - T_{f(i)}) + M_d\lambda_{v(i)}$	(5)
	$M_{d(i-1)}\lambda_{s(i)} + M_{b(i-1)}C_{p(i-1)}(T_{b(i-1)} - T'_{b(i)}) + \sum_{j=1}^{i-2} M_{d(j)}C_{p(j)}(T_{v(j)} - T'_{b(i)})$	(6)
	$= M_{f(i)}C_{p(i)}(T_{b(i)} - T_f) + M_d\lambda_{v(i)}$	
Energy balance in condenser	$Q = (M_f + M_{cw})C_p(T_f - T_{cw})$	(7)
Overall material balance of ejector	$M_s = M_m + M_{ev}$	(8)
Entrainment ratio	$R_\alpha = M_m/M_{ev}$	(9)
	$R_\alpha = 0.296 \left(\frac{P_m}{P_{ev}} \right)^{1.19} \left(\frac{P_m}{P_{ev}} \right)^{0.015} \left(\frac{PCF}{TCF} \right)$	(10)
	$PCF = 3 \times 10^{-7} (P_m)^2 - 0.0009 P_m + 1.6101$	(11)
	$TCF = 2 \times 10^{-8} (T_{ev})^2 - 0.0006 T_{ev} + 1.0047$	
Performance analysis	$GOR = \frac{m_d}{m_{steam}}$	(12)
	$PR = \frac{m_d \Delta h_{ref}}{m_h \Delta h_i}$	(13)
Concentration ratio of seawater	$CR = \frac{X_{b(n)}}{X_{f(1)}}$	(14)

Table 2
Thermodynamic losses of the proposed systems [29].

Parameters	Formulas	
non-equilibrium allowance	$NEA_{(i)} = \frac{33.0(T_{b(i-1)} - T_{b(i)})^{0.55}}{T_{v(i)}}$	(15)
	$NEA'_{(i)} = \frac{0.33(T'_{b(i-1)} - T_{v(i)})}{T_{v(i)}}$	(16)
Boiling point elevation	$BPE = AX + BX^2 + CX^3$	(17)
	$A = (8.325 \times 10^{-2} + 1.883 \times 10^{-4}T + 4.02 \times 10^{-6}T^2)$	(18)
	$B = (-7.625 \times 10^{-4} + 9.02 \times 10^{-5}T - 5.2 \times 10^{-7}T^2)$	
	$C = (1.522 \times 10^{-4} - 3 \times 10^{-6}T - 3 \times 10^{-8}T^2)$	(19)
Coal consumption variation	$\Delta B = \left(\frac{B_{coal}}{P} - \frac{B_{coal}}{P + \frac{(h_{c4} - h_{pq})M_{cq}}{1000}} \right) \times 1000$	

In order to avoid low temperature corrosion in the cases for exhaust flue gas heat recovery of the boiler, terminal flue gas temperature is set as 85 °C, which is higher than the acid dew point.

3.2. Economic analysis

The design of the new system needs to take into account the impact on water production costs, so it is necessary to carry out economic analysis. The water production cost is computed and the related equations are listed in Table 3.

The water production cost can be computed by the annualized capital cost and the annual operational cost as shown in Table 3. In which, C_{land} is land cost and it usually varies from place to place. It is assumed as zero in present study as land is available. C_{At} is the cost of total surface. i is the interest rate, n , is the number of years, f , is the plant load factor, C_{steam} is the price of motive steam, which is assumed to be 0 in scheme 1 and 2 since there is no motive steam. T_i and T_c are the evaporation and condensation temperature, respectively. The assumption values are listed in Table 4.

The economic analysis requires the calculation of heat transfer area. The equations of the vapor-seawater heat exchanger are listed in Table 5.

In order to calculate the area of all heat exchangers, the flue gas-seawater heat exchangers involved in this article use finned tube heat exchangers. The basic parameters are listed in Table 6. Assuming the

Table 3
Economic modeling of the proposed systems [31,32].

Parameters	Formulas	
The water production cost	$C_{\text{annual}} = \frac{C_{\text{cap}} + C_{\text{op}}}{f \cdot 365 \cdot D_{\text{fresh}}}$	(20)
Annualized capital cost	$C_{\text{cap}} = Z \cdot C_{\text{CAP}} + C_{\text{ins}}$	(21)
The total capital cost	$C_{\text{CAP}, \text{MED}} = C_d + C_i$	(22)
	$C_{\text{CAP}, \text{Mod}} = C_{\text{CAP}, \text{MED}} \left(0.31 + 0.4 \frac{A_{\text{mod}}}{A_{\text{MED}}} + 0.29 \frac{D_{\text{mod}}}{D_{\text{MED}}} \right)$	(23)
The direct capital cost	$C_d = C_{\text{eq}} + C_{\text{land}} + C_{\text{sd}}$	(24)
Equipment cost	$C_{\text{eq}} = 4 \cdot C_{\text{At}}$	(25)
Site development cost	$C_{\text{sd}} = 0.2 \cdot C_{\text{eq}}$	(26)
The indirect capital cost	$C_i = C_{\text{fr}} + C_{\text{co}} + C_{\text{ow}} + C_{\text{em}}$	(27)
The freight cost	$C_{\text{fr}} = 0.05 \cdot C_d$	(28)
The construction cost	$C_{\text{co}} = 0.15 \cdot C_{\text{eq}}$	(29)
The owner's cost	$C_{\text{ow}} = 0.1 \cdot C_{\text{eq}}$	(30)
The contingency cost	$C_{\text{em}} = 0.1 \cdot C_d$	(31)
The amortization factor	$Z = \frac{i \cdot (i + 1)^n}{(i + 1)^n - 1}$	(32)
The annual insurance cost	$C_{\text{ins}} = 0.1 \cdot C_{\text{cap}}$	(33)
The annual operational cost	$C_{\text{op}} = C_{\text{lab}} + 365 \cdot f \cdot D_{\text{fresh}} (w_{\text{aux}} C_{\text{elec}} + C_{\text{steam}} / \text{GOR} + C_{\text{main}} + C_{\text{chem}})$	(34)
The labor cost	$C_{\text{lab}} = 0.1 \cdot f \cdot 365 \cdot D_{\text{fresh}}$	(35)

Table 4
The assumption values of economic analysis.

Parameters	Units	Amounts
i	–	0.08
n	year	20
f	–	0.9
w_{aux}	kWh/m ³	1.5
C_{elec}	\$/kWh	0.15
C_{main}	\$/m ³	0.03
C_{chem}	\$/m ³	0.04
C_{steam}	\$/m ³	10

velocity of flue gas is 10 m/s, according to the mass flow rate of flue gas, the cross-sectional area of the flue is approximately 70 m².

For the flue gas-seawater evaporator, the vertical tube falling film model is used for calculation. The heat transfer coefficient is calculated by empirical relation present in Table 7.

4. Results with analysis

A 600 MW coastal coal-fired power generating unit in north China is selected as the object. The unit adopted low temperature multi-effect distillation (LT-MED) with thermal vapor compressor (TVC) to realize water-electricity cogeneration. The desalination system is parallel flow with six effects. TVC is set at the end of the fourth effect. There is a condenser behind the sixth effect to condense the second vapor produced in the last effect and preheat feed brine at the same time. The feed brine of first two effects is preheated by the condensed water from the first effect before flows into the effects. The heat source of the first effect is steam mixed by extraction from the turbine and low

Table 6
The structure dimensions of fin-tube heat exchanger.

Items	Unit	Amount
D_i	m	0.03
D_o	m	0.038
δ_f	m	0.002
S_f	m	0.1
S_1	m	0.5
S_2	m	0.5

temperature vapor generated in the fourth effect in TVC. The parameters of this TVC-MED system are listed in Tables 8 and 9.

To compare with this system, three kinds of water-electricity cogeneration schemes, indicated as Scheme 1, 2 and 3, are proposed in Section 3 of this paper. For the present power generating unit, the flow rate of exhaust flue gas of boiler can be utilized for seawater desalination is about 701 m³/s, of which the initial temperature is 125 °C and its outlet temperature leaving the desalination system is 85 °C.

4.1. Scheme 1-Flue gas as heat source with seawater preheated by vapor from last effect

For the original TVC-MED seawater desalination system, the temperature change of heat source is an isothermal process, top temperature of seawater is close to the temperature of the heat source. But exhaust flue gas is a sensible heat source. Hence, in order to increase the heat that can be supplied to seawater by the heat source, a major temperature difference is necessary. Because of the absence of dynamic steam as a heat source, there is no TVC in this scheme. The quadratic approximation method is adopted by using EES to maximize the PR.

Table 5
The heat transfer area model equations of the vapor-seawater heat exchanger [29].

Parameters	Formulas	
Heat transfer area of each evaporator	$A_i = \frac{Q_i}{U_i \cdot \text{LMTD}_i}$	(36)
Logarithmic mean temperature difference	$\text{LMTD} = \frac{(T_{h,\text{in}} - T_{c,\text{in}}) - (T_{h,\text{o}} - T_{c,\text{o}})}{\ln \frac{(T_{h,\text{in}} - T_{c,\text{in}})}{(T_{h,\text{o}} - T_{c,\text{o}})}}$	(37)
The overall heat transfer coefficient of evaporator	$U_i = (1939.4 + 1.40562T_i - 0.0207525T_i^2 + 0.0023186T_i^3) \cdot 10^{-3}$	(38)
The overall heat transfer coefficient of condenser	$U_c = (1617.5 + 0.1537T_c + 0.1825T_c^2 - 0.00008026T_c^3) \cdot 10^{-3}$	(39)

Table 7

The heat transfer coefficient of flue gas -seawater heat exchanger [33–35].

Parameters	Formulas
The heat transfer coefficient of two phase flow in vertical tube	$h_i = C_1 Co^{C_2} h_{li} + C_3 Bo^{C_4} h_{li}$ (40)
The liquid-only heat transfer coefficient	$h_{li} = 0.023 \frac{k_l}{D_i} Re_l^{0.8} Pr_l^{0.4}$ (41)
Convection number	$Co = \left(\frac{1}{x} - 1\right)^{0.8} \left(\frac{\rho_v}{\rho_l}\right)^{0.1}$ (42)
Boiling number	$Bo = \frac{q}{GA}$ (43)
Liquid Reynolds number	$Re_l = \frac{GD_l(1-x)}{\mu_l}$ (44)
The heat transfer coefficient of flue gas	$h_o = 0.251 \left(\frac{G_{max} D_o}{\mu}\right)^{0.67} \left(\frac{s_1 - D_o}{D_o}\right)^{-0.2} \left(\frac{s_1 - D_o}{s_f} + 1\right)^{-0.2} \left(\frac{s_1 - D_o}{s_2 - D_o}\right)^{0.4} \frac{k_y}{D_e}$ (45)
The overall heat transfer coefficient	$U_o = \frac{1}{\frac{1}{h_o} + \frac{D_o}{D_i} \frac{1}{h_i} + \frac{D_o}{k_{tube}} \ln \frac{D_o}{D_i} + R_{fi} + R_{fo}} \cdot 10^{-3}$ (46)

C_1 , C_2 , C_3 and C_4 are the constants, the values can refer to the literature. R_{fi} and R_{fo} are the fouling resistance inside and outside of the tube. The values are assumed as 0.0005 (m²·K)/W and 0.00086, respectively. k_{tube} is the thermal conductivity of tube, which is 208.4 W/(m·K).

Table 8

The operating temperatures of the TVC-MED system.

Items	Unit	1st	2ed	3rd	4th	5th	6th
Heating steam temperature	°C	65.0	61.5	58.3	55.1	52.1	49.1
Raw material temperature	°C	25	25	25	25	25	25
Feed brine temperature	°C	48.8	48.8	41.8	41.8	41.8	41.8
Boiling temperature	°C	61.7	58.4	55.3	52.3	49.3	46.0

Table 9

The property parameters and performance of the TVC-MED system.

Items	Unit	Amount
Raw material salinity	%	3.5
Discharge concentration	%	5.2
Concentration ratio		1.43
Fresh water production	m ³ /d	12,000
GOR		9.67

In the given scope of the exhaust flue gas temperature and the evaporating temperature of each effect, it is found that 2 times the amount of flue gas that the boiler can offer is needed to maintain the same freshwater production as that of the original TVC-MED system.

The maximum water production can be obtained by changing feed brine temperature of each effect and the mass flow rate of feed brine. When there is an equal mass flow rate of feed brine in each effect, the amount of output water can be increased with feed brine temperature. When the feed brine temperature is fixed, the increase in mass flow rate will lead to the reduction of the output water. The results are shown in Fig. 4.

As shown in Fig. 4, the increase of feed brine temperature makes the portion of heat needed for heating feed brine to boiling point reduced, and hence more heat can be used in seawater evaporation, then more second vapor and freshwater output can be obtained. It can be understanding the variation tendency in Fig. 2 by Eqs. (7) and (14). When the temperature of feed brine is fixed, the increase of feed flow rate leads to more heat needed for preheating seawater to saturation temperature, thus the total production will be declined. Therefore, the more the feed brine, the less second vapor in the last effect and thus the less amount of cooling water. The less the feed brine, the higher the concentration ratio. Restricted by scaling of equipment, concentration ratio is generally less than 2, thus the minimum feed brine flow rate is restricted by the concentration ratio. In addition, feed brine temperature is limited by the temperature and released heat of second vapor produced in the last effect. So when the amount of feed brine of each effect is specified, the higher the feed brine temperature, the less the need of cooling water.

When the thermal power plant is at the off-design condition, the mass flow rate and temperature of exhaust flue gas may change but the trend change between M_f and M_d , M_{cw} is consistent with Fig. 4.

The variations of water production and performance ratio with feed brine temperature can be observed in Fig. 5. Consistent with the trend in Fig. 4, it can be obtained that the performance ratio increases with feed brine temperature and water production. Restricted by scaling of equipment, concentration ratio is generally less than 2. Under this condition, the performance parameters of Scheme 1 are listed in Table 10 when the feed brine temperature is 42 °C.

While utilizing the exhaust flue gas as the heat source of the first effect, extracting steam from the turbine can be saved consequently, which increases the turbine work output about 10.75 MW. As a result, the coal consumption of power plant is reduced by about 6.05 g/kWh.

Fig. 6 shows the optimum water production and performance ratio of the desalination system under different operating conditions. The performance ratio is defined by Eq. (13). As the work output of the power plant is reduced, the mass flow rate and temperature of exhaust flue gas are reduced. Therefore, the water production is reduced. As the numerator and denominator in Eq. (13) are simultaneously reduced, the performance ratio of the desalination system can remain almost unchanged.

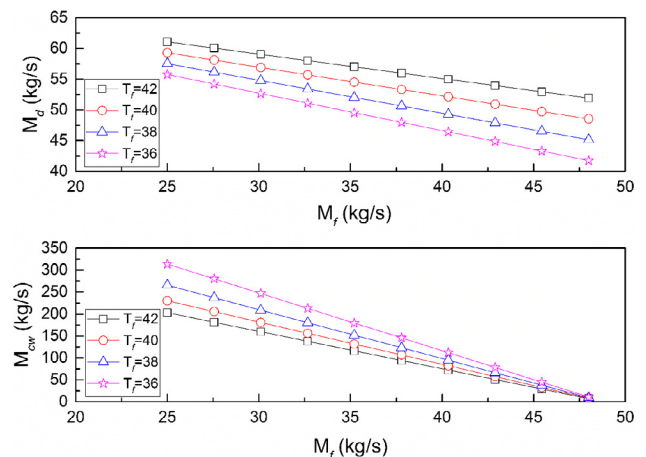


Fig. 4. Variation of total fresh water production and cooling water needed of Scheme 1 with feed brine flow rate and inlet feed brine temperature of each effect.

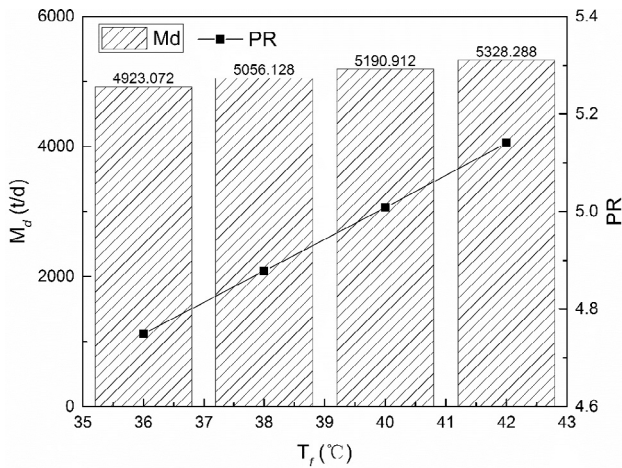


Fig. 5. Variations of water production and performance ratio of Scheme 1 with feed water temperature.

Table 10

The performance parameters of Scheme 1.

Items	Unit	Amount
Feed water temperature	°C	42
Mass flow rate of feed water in each effect	t/h	84.5
Fresh water production	m³/d	5328.3
mass flow rate of cooling water	t/h	777.96
Concentration ratio		1.78
PR		5.14
Coal consumption variation	g/kWh	6.05

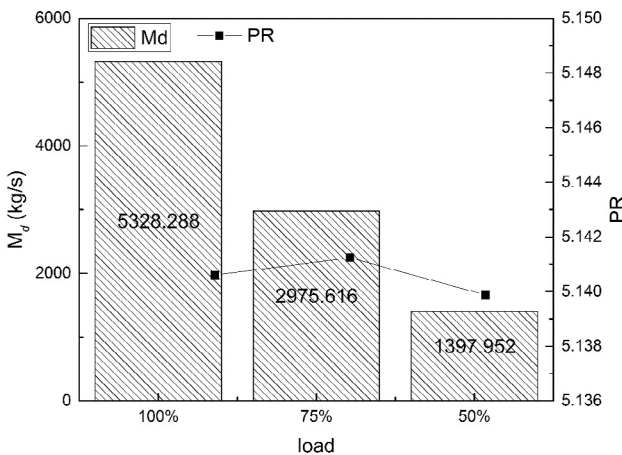


Fig. 6. Variations of the optimum water production and performance ratio of Scheme 1 with different operating conditions.

4.2. Scheme 2-Flue gas heat source with seawater preheated by exhaust steam and vapor from last effect

Use the exhaust flue gas as the heat source of the first effect, seawater that flows into the condenser is part of the circulating seawater in steam turbine condenser, which means that the seawater can be heated by the turbine exhaust steam and second vapor generated from the last effect successively, and then parallel flows into each effect.

When the feed brine mass flow rate is equal in each effect, the fresh water production increases with the feed brine temperature. On the other hand, when the feed water temperature is fixed, the increase in mass flow rate of feed brine decreases the fresh water production. Therefore more feed brine results in less second vapor in the last effect, and hence the cooling water needed for condenser declines. The results

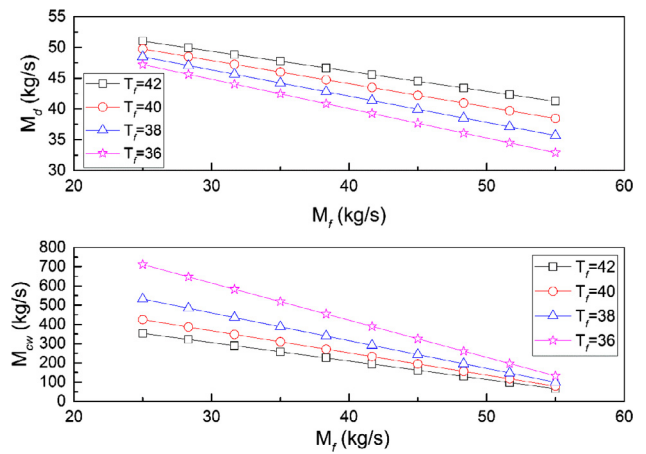


Fig. 7. Variation of total fresh water production and cooling water needed of Scheme 2 with feed brine flow rate and inlet feed brine temperature of each effect.

Table 11

The performance parameters of Scheme 2.

Items	Unit	Amount
Feed brine temperature	°C	42
Mass flow rate of feed water in each effect	t/h	84.49
Water output	m³/d	5328.29
Mass flow rate of cooling water	t/h	1320.84
Concentration ratio		1.78
PR		5.14
Coal consumption variation	g/kWh	6.05

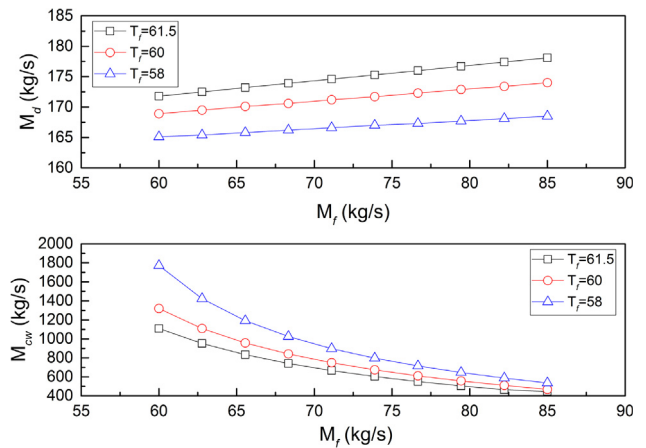


Fig. 8. Variation of total fresh water production and cooling water needed of Scheme 3 with feed brine flow rate and inlet feed brine temperature of each effect.

Table 12

The performance parameters of Scheme 3.

Items	Unit	Amount
Feed water temperature	°C	61.5
Mass flow rate of feed water in first four effects	t/h	300.24
Mass flow rate of feed water in last two effects	t/h	120.1
Water output	m³/d	15353.28
Mass flow rate of cooling water	t/h	1613.88
Concentration ratio		1.79
GOR		12.79

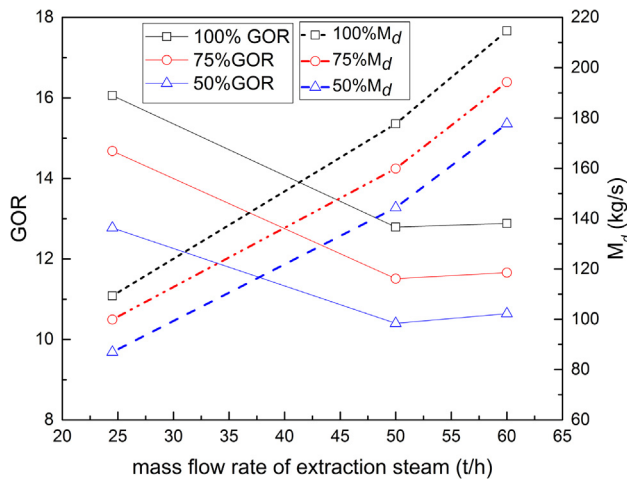


Fig. 9. Variations of water production and gain output ratio of Scheme 3 with extraction steam amount under different operating conditions.

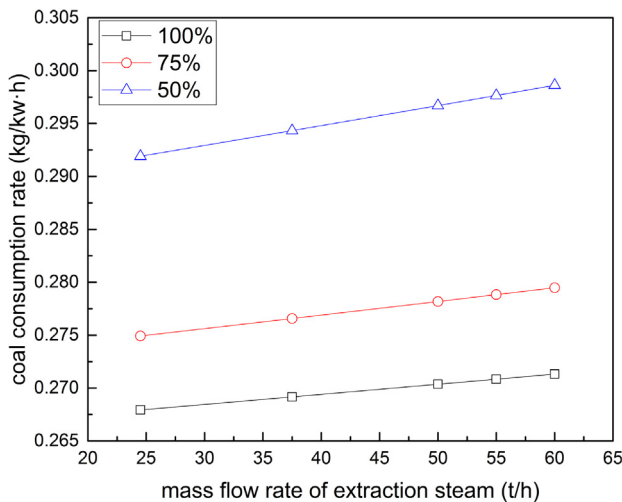


Fig. 10. Variations of coal consumption rate of Scheme 3 with extraction steam amount under different operating conditions.

Table 13

The economic results of the water-electricity cogeneration schemes.

Schemes	D_{fresh} (m ³ /d)	Water production cost (\$/m ³)
TVC-MED	12,000	3.14
Scheme 1	5328.288	2.19
Scheme 2	5328.288	2.19
Scheme 3	14342.4	2.43

Table 14

The parameters of the flue gas heating the condensate water.

Items	Description	Unit	Amount
T_y	Inlet flue gas temperature	°C	125
T'_y	Outlet flue gas temperature	°C	85
T_w	Inlet water temperature	°C	33.5
T'_w	Outlet water temperature	°C	84.8
ΔT_m	Logarithmic mean temperature difference	°C	45.62
ΔB	Decrement of net coal consumption	g/kWh	1.26

are shown in Fig. 7.

When the feed brine temperature is 42 °C, the performance parameters of Scheme 2 are listed in Table 11. It can be found that main

parameters are same as that of Scheme 1, except that the mass flow rate of cooling water needed is increased significantly.

In the present study, the feed brine is restricted to 42 °C even though the additional heat source is available to additionally preheat the feed brine. This is because that the seawater is preheated by the second vapor of the last effect in the condenser, and then flows into evaporators as feed brine. The feed brine temperature is restricted by the temperature of the second vapor of the last effect. In our proposed system, the evaporation temperature of the last effect is 46 °C, so the maximum feed brine temperature is restricted at 42 °C.

The main difference between Scheme 1 and Scheme 2 is that the temperature of seawater flows into condenser is elevated. The freshwater production of Scheme 2 equals to that of Scheme 1 is due to the temperature of effects are same and heat of the exhaust flue gas is specified. That is to say, the amount of heat released in the condenser by second vapor from the last effect is constant. Therefore when the feed brine temperature is the same, increasing the inlet seawater temperature can result in the increase of cooling water. Similarly, when using this system to obtain the same freshwater production as that of the original system, the main difference between Scheme 1 and Scheme 2 is that much more cooling water is needed in Scheme 2. Thus all parameters except the mass flow rate of cooling water are identical with that of Scheme 1.

4.3. Scheme 3-Extracting steam of turbine as heat source with seawater successively preheated by vapor from last effect, condensed water of first effect and exhaust flue gas of boiler

In this case, the fourth extracting vapor is used as the heat source just like that of the original LT-MED system. Also, TVC is set at the end of fourth effect. The feed brine is preheated by the second vapor of the last effect, the condensed water of first effect and the exhaust flue gas of boiler successively, by which it may be heated to the saturation point of the first effect under different working conditions. Because of the parallel feed flow configuration, the feed brine may be superheated relative to the rest effects, so that there is a flashing immediately when the feed brine flows into the rest effects, which increase the freshwater output greatly.

For Scheme 3, variations of fresh water production and cooling water with inlet feed brine temperature and flow rate are illustrated in Fig. 8. When the feed brine temperature is fixed, the increase of feed brine flow rate leads to the increment of fresh water production and reduction of cooling water needed.

It is obvious that the variation tendency of fresh water production and cooling water needed for Scheme 3 is different from that of Scheme 1 and 2. The main reason is the difference in feed brine temperature. The feed brine temperature in Scheme 1 and 2 is lower than the evaporation temperature of the corresponding evaporator, so a part of the heat is needed to heat the brine to saturation temperature. That is to say, with the increase of feed brine flow rate, more heat should be used for heating than that for evaporation, thereby reducing the amount of fresh water. In Scheme 3, due to the existence of multi-stage preheating, the feed brine can be heated to the saturation point of the first effect. As a result, more feed brine leads to more water production.

When the feed brine temperature is 61.5 °C, which is the saturation temperature of the first effect, the performance parameters of Scheme 3 are listed in Table 12. It can be found that the freshwater production is 1.28 times of that of the original TVC-MED system. Variations of water production and gain output ratio with the mass flow rate of extraction steam under different work conditions are shown in Fig. 9. Variations of coal consumption in the thermal power plant with the extraction steam amount under different work conditions are shown in Fig. 10.

In another way, it can be obtained the same freshwater production as that of the original TVC-MED system with 37.0 t/h extracting steam from turbine by Scheme 3. The extraction is 13.0 t/h, less than that of the original system, with which the consequent increase of turbine

power output is about 2.79 MW. It can be calculated as a reduction of the coal consumption about 1.42 g/kWh.

As shown in Fig. 9, the water production increases while the gain output ratio decreases with steam extraction. The reason is that the heat released from the steam is first used to heat seawater to the evaporation point before producing steam vapor, so there is a non-equalize rate of increase between the amount of extraction steam and water production.

4.4. Economic analysis results

The economic results of the proposed three schemes and the TVC-MED system are demonstrated in Table 13.

From the Table 13, it can be seen that TVC-MED has the highest water production cost, followed by scheme 3, and the scheme 1 and 2 have the lowest water production cost. This is mainly due to the high cost of motive steam. Therefore, although the use of flue gas as the heat source in scheme 1 and 2 reduces the water production, it also reduces the cost. In Scheme 3, the use of flue gas for preheating can increase the amount of water produced, and can also effectively reduce the water production cost.

4.5. Heating condensed water using flue gas

Flue gas can also be applied to heat condensed water if the GGH is canceled. Currently, the main way to recover the waste heat of exhaust flue gas for a coal-fired power plant is to install a low temperature economizer in the downstream of the flue. Thus, the heat of the exhaust flue gas can be recovered. The exhaust steam from the turbine is condensed and recycled back to the boiler as feed water after multistage preheating using steams extracted from the turbine. With the installation of low temperature economizer, part of the exhaust heat of the flue gas is recovered and used to heat the feed water, replacing a portion of the heat from the steam turbine. The saved steam can be able to pass through the steam turbine and expand for more output for power [36]. Here we calculated at the condition that low temperature economizer is in parallel with low temperature heat exchanger NO. 7 and 8. Condensed water is induced from the entrance of NO. 8 heat exchanger, and flows into NO. 6 heat exchanger after being heated in low temperature economizer.

For the sake of convenient to compare, assuming that flue gas is also cooled from 125 °C to 85 °C for heating water. The parameters and results are shown in Table 14.

Results showed that using low temperature flue gas to heat condensed water can theoretically reduce coal consumption 1.26 g/kWh.

5. Conclusions

Three schemes were proposed to combine the low grade heat in a 600 MW power generating unit with LT-MED seawater desalination. A six-effect TVC-MED system using extracting steam as the heat source was taken as contrast. The schemes were also compared with the case that flue gas was used to heat condensed water. The following conclusions can be obtained.

- (1) Freshwater production of Scheme 3 is the largest among all schemes proposed in this study. The water production is about 1.28 times of the original TVC-MED system. Freshwater production of Scheme 1 and Scheme 2 are all thousands of tons, less than that of the original TVC-MED system. However, because of the utilization of low temperature flue gas and the decrease of extracting steam from the turbine, an extra power output of 10.75 MW by the 600 MW power generating unit can be acquired, and the coal consumption of power generation is reduced about 6.05 g/kWh.
- (2) The feed brine temperature is restricted by the boiling temperature of the last effect. Therefore employing the circulating seawater of steam turbine condenser is meaningless in improving the water

production of MED system when the final effect vapor temperature and the heat source of the first effect is specified.

- (3) Economic analysis results showed that reduce the extract steam from the turbine can significantly reduce the water production cost. From the viewpoint of the impact on the power plant, the combination of exhaust flue gas and desalination system is better than that of heating condensed water.

On account of that seawater is part of the circulating cooling water in steam turbine condenser in Scheme 2, and the circulating water always is added with chlorine, which can influence the desalination equipment and the quality of fresh water, further analysis is needed in the practical applications.

Acknowledgement

The financial supports for this research project from the National Natural Science Foundation of China (No. 51676069) and the national “973 Program” of China (No. 2015CB251503) are gratefully acknowledged.

References

- [1] M. Al-Sahali, H. Ettouney, Developments in thermal desalination processes: Design, energy, and costing aspects, *Desalination* 214 (2007) 227–240.
- [2] M.W. Shahzad, M. Burhan, A. Li, K.C. Ng, Energy-water-environment nexus underpinning future desalination sustainability, *Desalination* 413 (2017) 52–64.
- [3] I.S. Al-Mutaz, I. Wazeer, Development of a steady-state mathematical model for MEE-TVC desalination plants, *Desalination* 351 (2014) 9–18.
- [4] H. Sayyaadi, A. Saffari, Thermoeconomic optimization of multi effect distillation desalination systems, *Appl. Energy* 87 (2010) 1122–1133.
- [5] R. Kouhikamali, M.M.M. Sanaei, Process investigation of different locations of thermo-compressor suction in MED-TVC plants, *Desalination* 280 (2011) 134–138.
- [6] B. Ortega-Delgado, P. Palenzuela, D.C. Alarcón-Padilla, Parametric study of a multi-effect distillation plant with thermal vapor compression for its integration into a Rankine cycle power block, *Desalination* 394 (2016) 18–29.
- [7] P. Fiorini, E. Sciubba, Modular simulation and thermoeconomic analysis of a multi-effect distillation desalination plant, *Energy* 32 (2007) 459–466.
- [8] I.S. Al-Mutaz, I. Wazeer, Comparative performance evaluation of conventional multi-effect evaporation desalination processes, *Appl. Therm. Eng.* 73 (2014) 1194–1203.
- [9] G. Qi, F. Jiang, Numerical investigation on prevention of fouling in the horizontal tube heat exchanger: Particle distribution and pressure drop, *Desalination* 367 (2015) 112–125.
- [10] A. Almulla, A. Hamad, M. Gadalla, Integrating hybrid systems with existing thermal desalination plants, *Desalination* 174 (2005) 171–192.
- [11] S. Manju, N. Sagar, Renewable energy integrated desalination: A sustainable solution to overcome future fresh-water scarcity in India, *Renew. Sustain. Energy Rev.* 73 (2017) 594–609.
- [12] Y.P. Min, S. Shin, E.S. Kim, Effective energy management by combining gas turbine cycles and forward osmosis desalination process, *Appl. Energy* 154 (2015) 51–61.
- [13] R. Deng, L. Xie, H. Lin, J. Liu, W. Han, Integration of thermal energy and seawater desalination, *Energy* 35 (2010) 4368–4374.
- [14] M.W. Shahzad, K. Thu, Y.D. Kim, K.C. Ng, An experimental investigation on MEDAD hybrid desalination cycle, *Appl. Energy* 148 (2015) 273–281.
- [15] H. Mokhtari, M. Sepahvand, A. Fasihfar, Thermoeconomic and exergy analysis in using hybrid systems (GT + MED + RO) for desalination of brackish water in Persian Gulf, *Desalination* 399 (2016) 1–15.
- [16] B. Rahimi, A. Christ, K. Regenauer-Lieb, T.C. Hui, A novel process for low grade heat driven desalination, *Desalination* 351 (2014) 202–212.
- [17] J.H. Reif, W. Alhalabi, Solar-thermal powered desalination: Its significant challenges and potential, *Renew. Sustain. Energy Rev.* 48 (2015) 152–165.
- [18] P. Palenzuela, G. Zaragoza, D.C. Alarcón-Padilla, Characterisation of the coupling of multi-effect distillation plants to concentrating solar power plants, *Energy* 82 (2015) 986–995.
- [19] V.G. Gude, Geothermal source potential for water desalination – current status and future perspective, *Renew. Sustain. Energy Rev.* 57 (2016) 1038–1065.
- [20] J. Bundschuh, N. Ghaffour, H. Mahmoudi, M. Goosen, S. Mushtaq, J. Hoinkis, Low-cost low-enthalpy geothermal heat for freshwater production: Innovative applications using thermal desalination processes, *Renew. Sustain. Energy Rev.* 43 (2015) 196–206.
- [21] G. Berding, F. Wilke, T. Rode, C. Haense, G. Joseph, G.J. Meyer, M. Mamach, M. Lenarz, L. Geworski, F.M. Bengel, Thermal desalination using diesel engine exhaust waste heat — An experimental analysis, *Desalination* 358 (2015) 94–100.
- [22] F. Zhang, S. Xu, D. Feng, S. Chen, R. Du, C. Su, B. Shen, A low-temperature multi-effect desalination system powered by the cooling water of a diesel engine, *Desalination* 404 (2017) 112–120.
- [23] F. Mahbub, M.N.A. Hawlader, A.S. Mujumdar, Combined water and power plant (CWPP) — a novel desalination technology, *Desalin. Water Treat.* 5 (2009)

- 172–177.
- [24] H.T. El-Dessouky, H.M. Ettouney, F. Mandani, Performance of parallel feed multiple effect evaporation system for seawater desalination, *Appl. Therm. Eng.* 20 (2000) 1679–1706.
- [25] G. Xu, S. Huang, Y. Yang, Y. Wu, K. Zhang, C. Xu, Techno-economic analysis and optimization of the heat recovery of utility boiler flue gas, *Appl. Energy* 112 (2013) 907–917.
- [26] C. Wang, B. He, S. Sun, Y. Wu, N. Yan, L. Yan, X. Pei, Application of a low pressure economizer for waste heat recovery from the exhaust flue gas in a 600MW power plant, *Energy* 48 (2012) 196–202.
- [27] Y. Zhong, X. Gao, W. Huo, H.T. Wang, Z.Y. Luo, M.J. Ni, K.F. Cen, Analysis of scaling on gas-gas heater surfaces of wet flue gas desulfurization systems, *J. Power Eng.* 02 (2008) 275–278 (in Chinese).
- [28] P. Han, X.J. Mao, S.M. Jiao, W.W. Ning, Advantages and disadvantages analysis with GGH in WFGD system, *Electric Power Sci. Eng.* (2006).
- [29] H.T. El-Dessouky, H.M. Ettouney, Fundamentals of salt water, *Desalination* (2002).
- [30] A. Christ, K. Regenauer-Lieb, T.C. Hui, Thermodynamic optimisation of multi effect distillation driven by sensible heat sources, *Desalination* 336 (2014) 160–167.
- [31] F.N. Alasfour, A.O. Bin, Amer, The feasibility of integrating ME-TVC + MEE with Azzour South Power Plant: Economic evaluation, *Desalination* 197 (2006) 33–49.
- [32] A. Christ, K. Regenauer-Lieb, H.T. Chua, Boosted multi-effect distillation for sensible low-grade heat sources: A comparison with feed pre-heating multi-effect distillation, *Desalination* 366 (2015) 32–46.
- [33] S.G. Kandlikar, A general correlation for saturated two-phase flow boiling heat transfer inside horizontal and vertical tubes, *J. Heat Transfer* 112 (1990) 219–228.
- [34] T. Kuppan, S.W. Qian, J.Y. Liao, X.H. Deng, X.M. Ma, Y. Feng, *Heat Exchanger Design Handbook*, 2004 (in Chinese).
- [35] J.F. Liu, *Theory and Design for Fin-Tube Heat Exchangers*, 2013 (in Chinese).
- [36] C. Wang, B. He, L. Yan, X. Pei, S. Chen, Thermodynamic analysis of a low-pressure economizer based waste heat recovery system for a coal-fired power plant, *Energy* 65 (2014) 80–90.